Available online at www.sciencedirect.com
ScienceDirect
Nuclear Science and Techniques 19 (2008) 53–57
NUCLEAR SCIENCE AND TECHNIQUES

Satellite-based detection of 16.76 MeV γ-ray from H-bomb D-T fusion

CHENG Jinxing[1,2,*] WANG Lan[2] OUYANG Xiaoping[2] SHI Jianfang[2] ZHANG Anhui[3]
SHEN Chunxia[3] OUYANG Maojie[1] NAN Qinliang[1]

[1] *Institute of Chemical Defence,PLA, Beijing 102205, China*

[2] *Northwest Institute of Nuclear Technology, Xi'an 710024, China*

[3] *Academy of Chemical Defence,PLA, Beijing 102205, China*

Abstract Based on the high energy γ-ray yield from the H-bomb D-T fusion reaction, it brings forward the idea applying the 16.76 MeV γ-ray to judge whether the H-bomb happens or not, and to deduce the explosion TNT equivalent accurately. The Monte Carlo N-Particle was applied to simulate the high energy γ-ray radiation characteristics reaching the geosynchronous orbit satellite, and the CVD diamond detector suit for the requirements was researched. A series of experiments were carried out to testify the capabilities of the diamond detector. It provides a brand-new approach to satellite-based nuclear explosion detection.

Key words H-bomb, D-T fusion, High energy γ-ray, CVD diamond detector, Satellite-based detection

CLC number O571.5

1 Introduction

During the process of H-bomb explosion, the D-T reaction releases determinative proportion of high energy γ-ray (16.76 MeV), which associates with the amount of tritium. The relationship can be used to check an H-bomb explosion and to extrapolate its TNT equivalent. In this paper, a numerical simulation is performed on the high energy γ-ray detected by the CVD diamond detector in a geosynchronous orbit (GEO) satellite. A series of tests were done to testify capabilities of the diamond detector. This is a new approach for satellite-based nuclear explosion detection.

2 γ-rays from the D-T fusion

Instantaneous γ-rays from H-bomb explosion can be categorized into two groups. The first group includes γ-rays less than 7 MeV. Generated from the fission reaction, they are unelastic scattered γ-rays and captured γ-rays by slow neutrons. The second group includes high energy γ-rays produced mainly in the D-T reaction of

$$D+T\rightarrow {}^{4}He + n + 17.6\ MeV \quad (1)$$

With a branching ratio of about 5×10^{-5}[1,2], another D-T reaction takes place

$$D+T\rightarrow {}^{5}He^{*}\rightarrow {}^{5}He + \gamma\ (16.76\ MeV) \rightarrow {}^{4}He+n \quad (2)$$

It is the 16.76 MeV γ-ray that is used for detecting H-bomb explosion and estimating the TNT equivalent by the branching ratio.

3 Simulation of the γ-ray transportation

Transportation of the 16.76 MeV γ-ray in the atmosphere and its interaction with atmospheric matter were simulated using MCNP4C. The radiation characterics, e.g. energy and time spectra detected by the GEO satellite are given.

3.1 Mathematics and physics model

3.1.1 Source spectrum model

For convenience, the γ-ray simulation was done

* Corresponding author. *E-mail address:* venuschengfh@126.com

Received date: 2006-12-24

with single energy of 16.76 MeV and time FWHM of 10 ns.

3.1.2 Space model of the transportation

The transportation space of 16.76 MeV γ-ray was Earth-centred 89 spherical surfaces. The earth radius is R_E=6400 km. The satellite is in the geosychronous orbit of 36 000 km to the Earth's surface. The coordinates are related to the cartesian system used by Monte Carlo N-Particle (MCNP), with the origin at the Earth's center and the *Z*-axis vertical (Fig.1).

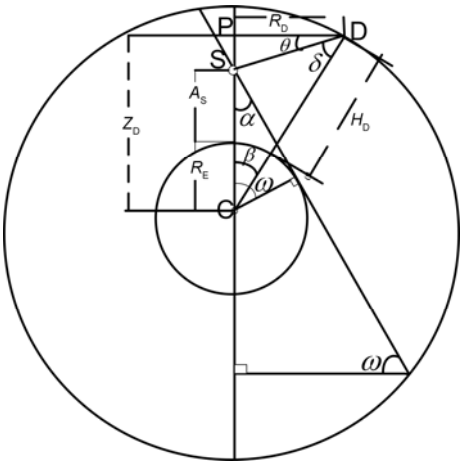

Fig.1 Geometrical relationships for ring-detector.

Because deep-penetration transport was not required, the only variance-reduction technique employed was MCNP ring-detector tallies. In this case, the source was placed in the atmosphere, and the detectors were located in a geosynchronous orbit at *R*g=42 400 km. The source altitude was respectively 30, 80 and 120 km.

The source S was located along the *Z*-axis at an altitude A_S above the Earth. We assumed that the detector *D* was in a circular orbit at height H_D above the Earth surface, and the source was in a slant angle of θ to the horizon. Because the geometry is symmetric about the *Z*-axis, the flux tallies could be obtained by placing an MCNP ring detector at the appropriate altitude Z_D and radius R_D. For each source altitude A_S, multiple detector heights H_D and slant angles θ could be tallied in a single MCNP run. The Z_D and R_D values needed for the MCNP tallies were calculated as follows

$$Z_D = (H_D + R_E)\cos\beta \tag{3}$$

$$R_D = (H_D + R_E)\sin\beta \tag{4}$$

Based on the cosine theorem

$$\frac{\sin(\pi/2+\theta)}{H_D+R_E} = \frac{\sin\delta}{A_S+R_E} \tag{5}$$

$$\beta + \frac{\pi}{2} + \theta + \delta = \pi \tag{6}$$

we obtain

$$\delta = \tan^{-1}\left\{\frac{(A_S+R_E)\sin(\pi/2+\theta)}{[(H_D+R_E)^2-(A_S+R_E)^2\sin^2(\pi/2+\theta)]^{1/2}}\right\} \tag{7}$$

By calculating the β, parameters of the ring detector were deduced.

3.1.3 Transportation matter model

Part of the γ-rays reaching the ground would be rebounded to the atmosphere and to the GEO satellite. We assumed that the soil in 1 m depth of the ground was well-proportioned, and that the atmosphere had a uniform, altitude-independent composition of 79.1% nitrogen, 20.4% oxygen, and 0.48% argon. These are similar to the standard composition given in Ref. [3], which is 78.08% N, 20.95% O, 0.93% Ar, and 0.034% trace elements. The air density varies exponentially with altitude. Fig.2 shows a set of density values taken from the standard atmosphere of Ref.[3].

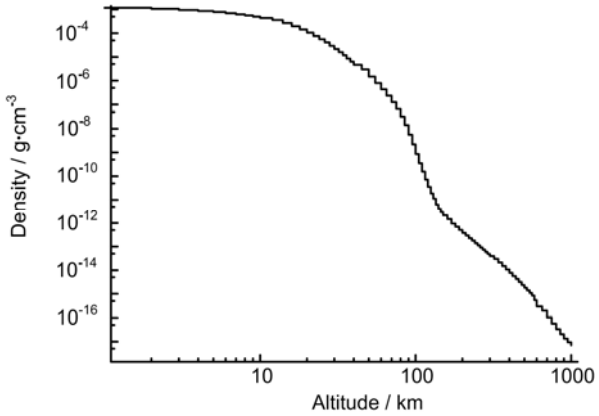

Fig.2 MCNP atmosphere histogram density.

3.2 Radiation characterics detected by the GEO

3.2.1 Energy spectrum characteristics

Fig.3 shows energy spectra of the 16.76 MeV γ-ray from the sources placed at altitude of 30, 80, and 120 km, respectively, and detected by the GEO satellite.

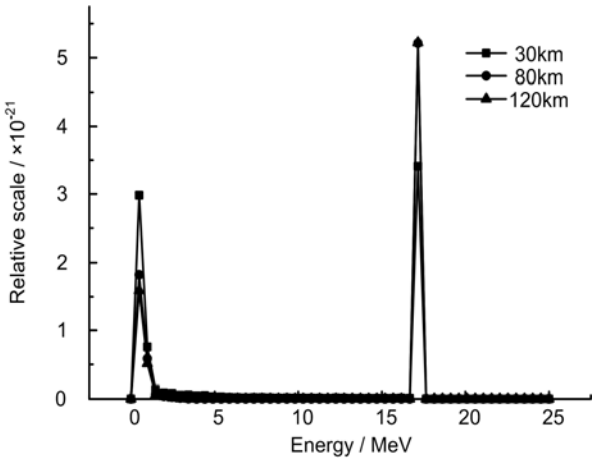

Fig.3 γ-ray energy spectra detected by GEO.

The peak at about 0.5 MeV in Fig.3 decreased in height with increasing source altitude.This is due to the effects of nitrogen nucleus de-excitation to low energy γ-rays. On the other hand, the peak height at 16.76 MeV increased with the altitude, with reduced energy spread width.

3.2.2 Time spectrum characteristics

Fig.4 shows time spectra of the 16.76 MeV γ-ray. Of course, the γ-ray from a source at a higher altitude reaches the satellite earlier.

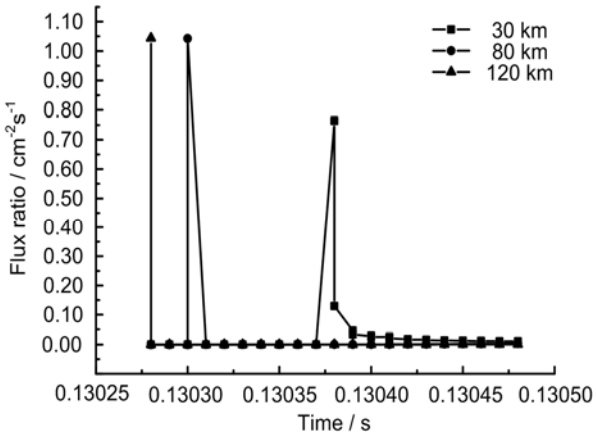

Fig.4 Time spectra of 16.76 MeV γ-ray.

4 Detection of the γ-ray and detector

4.1 Theory of high energy γ-ray detection

A γ photon interacts with matter *via* photoelectric absorption, Compton scattering, and electron pair production[4]. At such a high energy region, however, only electron pair production plays an important role. As the D-T fusion releases 7 MeV and lower energy γ-rays from de-excitation nitrogen nucleus, theseγ-rays must be eliminated from the background for measuring the 16.76 MeV γ-ray.

4.2 Sensitivity of high energy γ-ray detector

From theoretical simulation, peak intensity of the 16.76 MeV γ-ray is about 5×10^{7}~5×10^{9} $cm^{-2}\cdot s^{-1}$ in an explosion in the TNT equivalent of 0.01~1 million ton. Supposing that 100 nA electrical current be recordable, the sensitivity will be about 2×10^{-17}~2×10^{-15} $C\cdot cm^{2}$.

4.3 Diamond detector

Chemical vapor deposition (CVD) technique was developed in the 1990's. Detectors made of CVD diamond are featured by their low dark current, fast time response, hard radiation and heat resistance. An investigation[5] shows that, after irradiating a CVD diamond detector to about 1.4×10^{6} Gy in a ^{60}Co source (3.5×10^{14} Bq, 15 cm away) for 500 hours, no changes were observed in its dark current and sensitivity. And the detectors are used by the RD42 group[6] to detect 25.4 GeV/c pions in LHC (Large Hadron Collider) in CERN. CVD diamond detectors give a high signal noise ratio (SNR) because the dark current is less than 10 nA, 10^{-3} times of Si and other detectors, with sensitivity similar to the others. Therefore CVD diamond detector is a proper device for satellite-based detection.

We have developed the sandwich type diamond detector without junction[7]. The following sections report our research progress with the detector.

4.3.1 CVD diamond detector

The CVD diamond detector (no p-n junction) is in a metal-diamond–metal structure. Ti-Pt-Au contacts were thermally evaporated on two faces. The sensitive body is Φ45 mm×135 μm.

When a high energy photon excites electron pair, electric signals will be induced. As CVD diamond is spathic and not pure, there are accessional energy levels in the forbidden bond which consist of traps in diamond. Most of electrons and holes are trapped before they reach the electrodes. This determines the charge collection efficiency. By increasing the electric field, the carrier velocity[8] and charge collection efficiency increase and reach a saturation.

4.3.2 Stability of the CVD diamond detector

The sensitivity test was performed at the standard ^{60}Co source calibration lab in the Northwest Institute of Nuclear Technology. As shown in Fig.5, the sensitivity of the CVD diamond detector to 1.25 MeV γ-ray increased with the electric field and saturated at 2.5 V·μm^{-1}, with a saturated sensitivity of 2.5×10^{-18} C·γ^{-1}. The charge collection efficiency was as high as 60%. With increased sensitive area and thickness of the detector, the sensitivity can be 10^{-16}~10^{-17} cm^2·C, which well accord with the requirements of satellite-based detection.

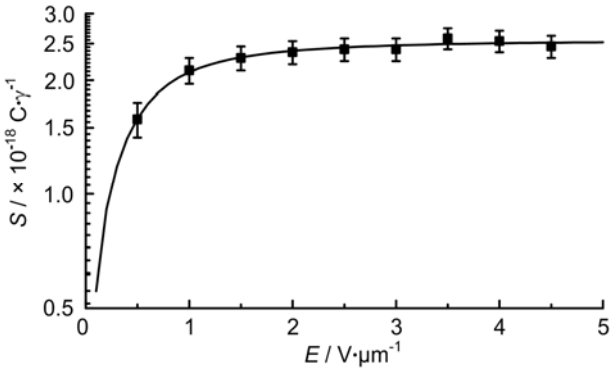

Fig.5 Sensitivity of diamond detector (the real line is from theoretical calculation).

4.3.3 Response to pulsed radiations of the CVD diamond detector

The detector's response to pulsed radiations was tested on "Qiang Guang I" device (Fig.6). The waveform from CVD diamond detector was consistent with the one from photoelectric tube. As a photoelectric tube is faster than a CVD diamond detector, it can distinguish the first two peaks and more factually reflects the original pulse. The waveform from CVD detector does not show the first two peaks as clearly as the photoelectric tube, but the low peak is shown better than photoelectric tube, because the CVD diamond detector has virtually no tail (see the time response test). For the irradiation test by the ^{60}Co γ-rays, the intensity at the detector (about 1.2 m away from the source and 5^o from the central axi) was 1.6×10^9 MeV/cm^2. Because the intensity attenuation and its anglar distribution were not perfect enough, we just concluded that the dose was 55 Gy in the detector in principle.

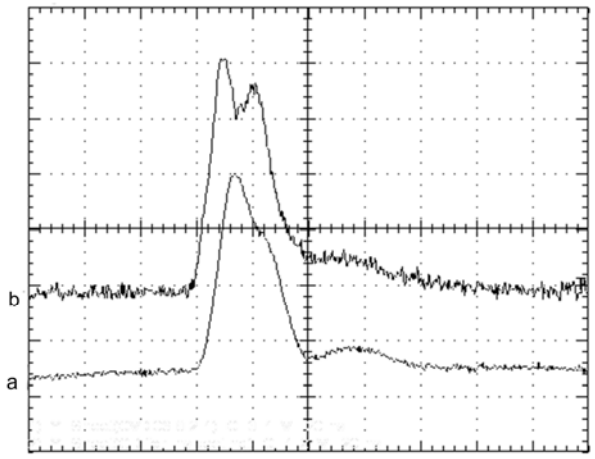

Fig.6 Waveform on "Qiang Guang I" from CVD diamond detector (a) and from photoelectric tube (b).

4.3.4 Time response of CVD diamond detector

Time response of the CVD diamond detector was tested on the *fs* pulsed UV source. Deducting from the acquisition system with 4 GHz bandwidth, rise time of the *Φ*50 mm×135 μm detector was 2.02 ns and the FWHM was 21 ns, which is identical with theoretical calculation (Fig.7). Its time response is much faster than Si-PIN detector of the same size.

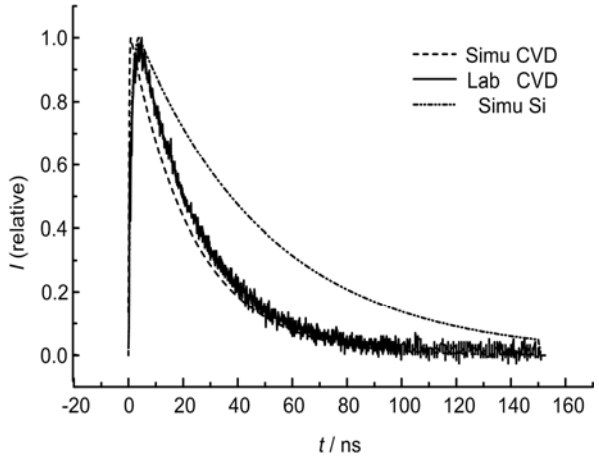

Fig.7 Time response on a fs UV source (the slick real is theoretic result of diamond detector; the flocky one is the test result of diamond detector; the dashed line is the theoretic result of Si-PIN detector with the same size).

5 Conclusion

From the theory and tests, we can see that satellite-based detection of high energy γ-ray is a very brand-new approach to identify H-bomb and to estimate the explosion TNT equivalent. The capabilities of CVD diamond detector are outstanding. We look forward to applying this method to provide a

good expectation in nuclear explosion detection field.

References

1 Glebov V Y, Meyerhofer D D, T C Sangster, *et al.* Rev Sci Instrum, 2006, **77:** 10E715.

2 Morgan G L, Lisowski P W, Wender S A, *et al.* Phys Rev C, 1986, **33:** 1224－1227.

3 Du H, Ye Z H. Space environments handbook of low orbit spacecraft. Beijing: National Defense Industry Press, 1996, 20-60.

4 Glenn F K. Radiation detection and measurement. New York: John Wiley & Sons, 1979, 15-30.

5 Bergonzo P, Brambilla A, Tromson D, *et al.* Nucl Instrum Methods Phys Res A, 2002, **476:** 694-700.

6 Tapper R J. Rep Prog Phys. 2000, **63:** 1273-1316.

7 Ouyang X P, Wang L, Fan R Y, *et al.* Chinese Physics, 2006, **55:** 2170-2174.

8 Pan L S, Han S, Kania D R, *et al.* J.Appl.Phys, 1993, **74:** 1086-1095.